

# Optimal molecular alignment and orientation through rotational ladder climbing

Julien Salomon\*

*Laboratoire Jacques-Louis Lions, Université Pierre & Marie Curie,  
Boîte courrier 187, 75252 Paris Cedex 05, France*

Claude M. Dion†

*Department of Physics, Umeå University, SE-901 87 Umeå, Sweden*

Gabriel Turinici‡

*INRIA Rocquencourt, B.P. 105, 78153 Le Chesnay Cedex and  
CERMICS-ENPC, Champs-sur-Marne,  
77455 Marne-la-Vallée Cedex, France*

(Dated: May 24, 2019)

## Abstract

We study the control by electromagnetic fields of molecular alignment and orientation, in a linear, rigid rotor model. With the help of a monotonically convergent algorithm, we find that the optimal field is in the microwave part of the spectrum and acts by resonantly exciting the rotation of the molecule progressively from the ground state, i.e., by rotational ladder climbing. This mechanism is present not only when maximizing orientation or alignment, but also when using prescribed target states that simultaneously optimize the efficiency of orientation/alignment and its duration.

## I. INTRODUCTION

External fields can be used to manipulate molecules, for instance by controlling their external angular degrees of freedom, to achieve, e.g., alignment (molecular axis parallel to a laboratory-fixed axis, such as the field polarization vector) or orientation (molecular axis is set to have the same direction as the laboratory-fixed axis). These two goals have a wide range of applications in fields such as chemical reactivity,<sup>1</sup> surface processing,<sup>2,3</sup> nanoscale design,<sup>4,5</sup> attosecond pulse production,<sup>6,7</sup> and quantum information processing.<sup>8</sup> For a recent review of the subject and of the methods used to achieve alignment and orientation, see Ref. 9.

The purpose of the present study is to find the electromagnetic fields that produce the best possible orientation or alignment. We start by presenting in Sec. II the rigid rotor model used to describe the rotation of a linear molecule, along with the cost functionals that describes the required control objectives, in terms of both observables measuring orientation or alignment and target states that embody the efficiency of orientation/alignment along with its persistence.

The optimization procedure itself is based on monotonically convergent algorithms<sup>10,11,12</sup> that are guaranteed to improve at each step the cost functional chosen. The discretized version of these algorithms is presented in Sec. II C.

As we will see in Sec. III, the fields leading to optimal orientation and alignment are in the microwave part of the spectrum and lead to *rotational ladder climbing*, i.e., the molecule is resonantly excited successively from one rotational level to the next. The possibility of controlling rotational excitation by ladder climbing using microwave fields was first proposed by Judson *et al.*<sup>13,14</sup> A process similar but resting on Raman excitation of ro-vibrational states with chirped pulses has been used to create an optical centrifuge for molecules.<sup>15,16,17,18,19</sup>

## II. MODEL

### A. Time-dependent Schrödinger equation

The dynamics of the molecule interacting with the electromagnetic field is obtained by solving the time-dependent Schrödinger equation (TDSE). We restrict ourselves to the case of a linear molecule in a rigid rotor approximation, yielding the Hamiltonian (in atomic

units,  $\hbar = 1$ )

$$\hat{H} = B\hat{J}^2 - \mu_0\mathcal{E}(t)\cos\theta - \left[(\alpha_{\parallel} - \alpha_{\perp})\cos^2\theta + \alpha_{\perp}\right]\frac{\mathcal{E}^2(t)}{2}, \quad (1)$$

where  $B$  is the rotational constant,  $\hat{J}$  is the angular momentum operator,  $\theta$  is the polar angle positioning the molecular axis with respect to the polarization vector of the linearly polarized electric field of amplitude  $\mathcal{E}(t)$ ,  $\mu_0$  is the permanent dipole moment, and  $\alpha_{\parallel}$  and  $\alpha_{\perp}$  are the dipole polarizability components parallel and perpendicular to the molecular axis, respectively. Because of the cylindrical symmetry about the field polarization axis, the motion associated with the azimuthal angle can be separated and  $M$ , the projection of the total angular momentum  $J$  on the axis, is a good quantum number ( $\Delta M = 0$ ). The TDSE (1) is solved numerically starting from the ground rotational (isotropic) state  $J = M = 0$ , using a basis set expansion of the wave function  $\psi$  in terms of the spherical harmonics  $Y_{J,M}$ ,

$$\psi(\theta, t) = \sum_{J=0}^{\infty} c_J(t)Y_{J,0}(\theta), \quad (2)$$

the  $c_J$  being complex coefficients and the coupling terms due to  $\mu_0$  and  $\alpha$  being then analytical.<sup>20</sup> For computational purposes, only the first 10 terms in the sum in Eq. (2) are kept, and we have checked that the results are not affected by using a bigger basis.

Because of the presence of both the dipole moment  $\mu$  and the polarizability anisotropy  $\Delta\alpha \equiv \alpha_{\parallel} - \alpha_{\perp}$ , the results are not molecule-independent. However, the role of the polarizability is negligible for the fields obtained, making them applicable to any linear molecule with a proper scaling of the amplitude and frequency of the electric field. The results will thus be presented with time expressed in units of the rotational period  $T_{\text{rot}} = h/2B$ , the electrical field as  $\mu_0\mathcal{E}/B$ , and energy as  $E/B$ . The parameters actually used in the calculations are those for the HCN molecule:  $B = 6.6376 \times 10^{-6}$ ,  $\mu = 1.1413$ ,  $\alpha_{\parallel} = 20.055$ , and  $\alpha_{\perp} = 8.638$  (all in atomic units).

## B. Cost functional

As we are seeking to optimize molecular orientation or alignment, our cost functionals are based on their respective measure, the expectation values  $\langle\cos\theta\rangle$  and  $\langle\cos^2\theta\rangle$ . A molecule will be oriented when  $|\langle\cos\theta\rangle| \sim 1$ , with the sign indicating in which direction it is pointing; an angular distribution symmetric with respect to  $\theta = \pi/2$  will yield a value of zero. The

expectation value of  $\cos^2 \theta$  is 1 when the molecule is aligned, starting from 1/3 for the isotropic case.

The first case we consider is a cost functional of the form

$$\mathcal{J}_1(\mathcal{E}) = \langle \psi(T) | \hat{O} | \psi(T) \rangle - \int_0^T \lambda(t) \mathcal{E}^2(t) dt, \quad (3)$$

with  $\hat{O}$  an operator chosen to be  $\cos \theta + \hat{I}$  for orientation and  $\cos^2 \theta + \hat{I}$  for alignment, the identity operator  $\hat{I}$  being used for convenience (e.g., it ensures that  $\hat{O}$  is positive) without modifying the extrema of  $\mathcal{J}_1$ , and  $T$  the time at which the interaction with the field ends. The last term in Eq. (3) is a penalization on the amplitude of the field, with

$$\lambda(t) = 10^5 \left( \frac{t - T/2}{T/2} \right)^6 + 10^4. \quad (4)$$

In addition to limiting the total fluence, such a form ensures a smoother, and thus more realistic, turn-on and turn-off of the field.

The downside of such a cost functional is that it takes into account only the efficiency of the orientation/alignment, not its persistence. Once the field is turned off, the free rotation of the molecule will lead to the disappearance of the orientation/alignment as the different  $J$  components in the wave function dephase, followed by revivals at intervals of one rotational period.<sup>21</sup> The best orientation/alignment is obtained by confining the molecule to a narrow angular distribution  $\Delta\theta$ , which corresponds to exciting a broad rotational band  $\Delta J$  by referring to an uncertainty principle  $\Delta J \cdot \Delta\theta \sim \hbar$ .<sup>9</sup> The problem is then that, conversely, a broad rotational spectrum exhibits narrow features in the time domain, i.e., the greater the orientation/alignment, the shorter its duration. A compromise has thus to be made, as can be achieved by considering the best orientation/alignment possible for a restricted maximum rotational excitation. The procedure on how states with such characteristics can be obtained is given in detail in Refs. 22,23, where it can also be seen that  $J_{\max} = 4$  offers a good compromise, leading to an orientation of  $\langle \cos \theta \rangle \approx 0.906$  or an alignment of  $\langle \cos^2 \theta \rangle \approx 0.837$ , both lasting of the order of 1/10th of the rotational period. The cost functional is now

$$\mathcal{J}_2(\mathcal{E}) = 2\Re \langle \psi_{\text{target}} | \psi(T) \rangle - \int_0^T \lambda(t) \mathcal{E}^2(t) dt, \quad (5)$$

where  $\psi_{\text{target}}$  denotes the target state corresponding to orientation or alignment, as given in Tab. I, and  $\Re$  the real part. Note that because of the norm conservation properties of the

Schrödinger equation, the cost functional (5) has the same minima and critical points as

$$\mathcal{J}(\mathcal{E}) = -\|\psi_{\text{target}} - \psi(T)\|^2 - \int_0^T \lambda(t) \mathcal{E}^2(t) dt, \quad (6)$$

which measures the distance between  $\psi_{\text{target}}$  and  $\psi(T)$ .

In all cases, the time at which the field is turned off and the cost functional measured is chosen as  $T = 9.5 \times 10^6$  a.u.  $\approx 20T_{\text{rot}}$  for the results presented here. Shorter durations lead to results either similar or less significant.

### C. Monotonically convergent algorithm

The algorithm used to find the optimal field is based on a general class of monotonically convergent algorithms recently proposed.<sup>12</sup> We present here the algorithm associated to  $\mathcal{J}_1$  and refer the reader to Refs. 24,25 for a detailed discussion the algorithm in a time-discretized framework. At the maximum of the cost functional  $\mathcal{J}_1$ , the Euler-Lagrange critical point equations are satisfied; a standard way to write these equations is to use a Lagrange multiplier  $\chi(\theta, t)$  called *adjoint state*. The following critical point equations are thus obtained:

$$\begin{aligned} i\partial_t \psi &= \hat{H}\psi, & \psi(0) &= \psi_0, \\ i\partial_t \chi &= \hat{H}\chi, & \chi(T) &= \hat{O}(\psi(T)), \\ \lambda(t)\mathcal{E}(t) &= -\Im \langle \chi | \mu_0 \cos \theta + 2\mathcal{E}(t) (\Delta\alpha \cos^2 \theta + \alpha_{\perp}) | \psi \rangle, \end{aligned} \quad (7)$$

where  $\Im$  is the imaginary part of a complex number and  $\psi_0$  the initial state of the controlled system.

Given two fields  $\mathcal{E}$  and  $\mathcal{E}'$  and the corresponding states  $\psi$ ,  $\psi'$  and adjoint states  $\chi$ ,  $\chi'$  defined by Eq. (7), one can write

$$\begin{aligned} \Delta\mathcal{J}_1 &= \mathcal{J}_1(\mathcal{E}') - \mathcal{J}_1(\mathcal{E}) \\ &= \langle \psi'(T) - \psi(T) | \hat{O} | \psi'(T) - \psi(T) \rangle \\ &\quad + \int_0^T [\mathcal{E}'(t) - \mathcal{E}(t)] \left\{ 2\Im \langle \psi'(t) | \mu_0 \cos \theta | \chi(t) \rangle \right. \\ &\quad \left. + [\mathcal{E}'(t) + \mathcal{E}(t)] \left[ 2\Im \langle \psi'(t) | \frac{\Delta\alpha \cos^2 \theta + \alpha_{\perp}}{2} | \chi(t) \rangle - \lambda(t) \right] \right\} dt. \end{aligned} \quad (8)$$

The first term of this sum is positive since both choices  $\hat{O} = \cos + \hat{I}$  or  $\hat{O} = \cos^2 + \hat{I}$  are positive. Given  $\mathcal{E}$ , the integrand provides thus an implicit criterion in terms of  $\mathcal{E}'$ , the

satisfaction of which guarantees the positivity of  $\Delta\mathcal{J}_1$ . An explicit choice of  $\mathcal{E}'$  can be exhibited: the integrand of Eq. (8) is a second-order polynomial with respect to  $\mathcal{E}'$  and for a large enough value of  $\lambda(t)$  the coefficient  $\Im\langle\psi'(t)|\frac{\Delta\alpha\cos^2\theta+\alpha_\perp}{2}|\chi(t)\rangle - \lambda(t)$  of  $\mathcal{E}'^2(t)$  is negative. It has thus a unique maximum, given by the cancellation of the derivative. The value obtained by this method is

$$\mathcal{E}'(t) = -\frac{\Im\langle\psi'(t)|\mu_0\cos\theta|\chi(t)\rangle}{2\Im\langle\psi'(t)|\frac{\Delta\alpha\cos^2\theta+\alpha_\perp}{2}|\chi(t)\rangle - \lambda(t)}. \quad (9)$$

The algorithm derived from the previous computations is then given by the following procedure: given at step  $k$  a field  $\mathcal{E}^k$  and its associated state  $\psi^k$  and adjoint state  $\chi^k$ , compute simultaneously  $\mathcal{E}^{k+1}$ ,  $\psi^{k+1}$  by

$$\begin{cases} \mathcal{E}^{k+1} = -\frac{\Im\langle\psi^{k+1}(t)|\mu_0\cos\theta|\chi^k(t)\rangle}{2\Im\langle\psi^{k+1}(t)|\frac{\Delta\alpha\cos^2\theta+\alpha_\perp}{2}|\chi^k(t)\rangle - \lambda(t)}, \\ i\partial_t\psi^{k+1} = \left[B - \mu_0\mathcal{E}^{k+1}(t)\cos\theta - \frac{[\mathcal{E}^{k+1}(t)]^2}{2}(\Delta\alpha\cos^2\theta + \alpha_\perp)\right]\psi^{k+1}, \\ \psi^{k+1}(0, \theta) = \psi_0(\theta). \end{cases} \quad (10)$$

Then compute backward evolution of  $\chi^{k+1}$  by

$$\begin{cases} i\partial_t\chi^{k+1} = \left[B - \mu_0\mathcal{E}^{k+1}(t)\cos\theta - \frac{[\mathcal{E}^{k+1}(t)]^2}{2}(\Delta\alpha\cos^2\theta + \alpha_\perp)\right]\chi^{k+1}, \\ \chi^{k+1}(T, \theta) = \hat{O}(\psi^{k+1}(T, \theta)). \end{cases} \quad (11)$$

The arguments above show that

$$\mathcal{J}_1(\mathcal{E}^{k+1}) \geq \mathcal{J}_1(\mathcal{E}^k). \quad (12)$$

### III. RESULTS

#### A. Optimizing orientation

The electric field obtained using the cost functional  $\mathcal{J}_1$  [Eq. (3)] with the observable  $\hat{O} = \cos\theta + \hat{I}$ , i.e., for the optimization of the orientation, is given in Fig. 1(a). To better analyze the result, we have performed a short-time Fourier transform (STFT),<sup>26</sup>

$$\mathcal{F}(\nu, t) = \int_{-\infty}^{+\infty} \mathcal{E}(\tau)w(\tau - t)e^{-i2\pi\nu\tau}d\tau, \quad (13)$$

where  $w$  is a Tukey-Hanning window with a temporal width of  $1.9 \times 10^6$  a.u. The frequency distribution  $\mathcal{F}$  can be seen in Fig. 1(b), where the abscissa is the dimensionless value  $2\nu T_{\text{rot}}$ ,

corresponding to the dimensionless energy  $E/B$ . The energy spacing between rotational states  $J$  and  $J + 1$  being  $2BJ$ , we see clearly from Fig. 1(b) that the field is initially resonant with the  $J = 0 \rightarrow 1$  transition, and subsequently comes in resonance with higher and higher pairs of rotational levels  $J = 1 \rightarrow 2$ ,  $J = 2 \rightarrow 3$ ,  $\dots$ . Looking at the population of the rotational states, in Fig. 2, we indeed find that, starting from the ground state  $J = 0$ , the molecule is pumped to the first excited state, then to the second, etc. At the end of interaction with the field, the population distribution is such that an orientation of  $\langle \cos \theta \rangle (T) = 0.909$  is attained (Fig. 3). In other words, the molecule is oriented by a process of *rotational ladder climbing*.

If we instead take the cost functional  $\mathcal{J}_2$  [Eq. (5)] with  $\psi_{\text{target}}$  the target state for orientation given in Tab. I, we obtain a result very similar to the previous one, as shown in Fig. 4. The main difference is the absence of the frequency component at  $2\nu T_{\text{rot}} = 10$ , which is easily understood from the fact that it corresponds to the  $J = 4 \rightarrow 5$  transition, while the target is restricted to  $J_{\text{max}} = 4$ . The resulting dynamics of  $\langle \cos \theta \rangle$  are nearly indistinguishable, as is seen in Fig. 5. The similarity of both results can also be explained by looking at the projection on the target  $P \equiv |\langle \psi_{\text{target}} | \psi(T) \rangle|^2$ . For the wave function obtained for the optimization of the observable, we already have  $P = 0.9933$ , the optimization of the projection on the target allowing to reach  $P = 0.9969$ . This efficiency is better than that obtained when kicking the molecule with short pulses.<sup>22,27</sup>

## B. Optimizing alignment

The result for the maximization of the operator  $\hat{O} = \cos^2 \theta + \hat{I}$  to achieve alignment is given in Fig. 6. The field obtained is almost the same as the one obtained for orientation, except that the rotational excitation happens at a quicker pace, as displayed in Fig. 7, where it is seen that  $J = 5$  is now significantly populated. The alignment obtained is  $\langle \cos^2 \theta \rangle = 0.866$ .

Changing now the target state for alignment (Tab. I), we see in Fig. 8 that the field obtained is significantly different. The frequency component corresponding to an energy of  $E = 4B$  is present for a longer time and components at  $E = 6B$  and, to a lesser extent,  $E = 2B$ , reappear near the turn-off of the field. The time dependence of the population of the rotational states in Fig. 9 gives the explanation of this phenomenon: the populations of  $J = 1$  and  $3$  are *pumped down* by these later components, since only even  $J$  levels are

populated in the optimally aligned target state. The original excitation to the odd levels was necessary as the rotational states are only significantly coupled via the permanent dipole moment, implying the selection rule  $\Delta J = \pm 1$ , the role of the polarizability being here negligible. This excitation-deexcitation scheme leads to a projection on the target state of  $P = 0.9950$ , compared with  $P = 0.5487$  when only optimizing for alignment.

It is interesting to note that the maximum alignment obtained is the same as in the first case, with  $\langle \cos^2 \theta \rangle (T) = 0.867$  (Fig. 10), even though the two wave functions obtained involve very different mixtures of spherical harmonics. One striking contrast between the two is actually not visible when looking only at  $\langle \cos^2 \theta \rangle$ : in the second case, the state obtained is *strictly* aligned, in the sense that the angular distribution is symmetric with respect to  $\theta = \pi/2$ . In the first case, the maximum in alignment corresponds also to a maximum in orientation, with  $\langle \cos \theta \rangle (T) = 0.891$ , whereas in the second case  $\langle \cos \theta \rangle (T) = -0.027$ .

#### IV. CONCLUSION

Using a monotonically convergent algorithm, we have searched for the optimal electric field maximizing either the alignment or the orientation of a linear molecule, taken in a rigid rotor approximation. We have carried out the optimization both in terms of maximization of observables corresponding to orientation/alignment and using target states offering a good compromise between the efficiency of orientation/alignment and its duration.

We have found that the optimal fields allow to reach orientation/alignment by rotational ladder climbing, i.e., by successive resonant excitation of neighboring rotational levels. This process allows to reach an orientation of  $\langle \cos \theta \rangle = 0.909$  or an alignment of  $\langle \cos^2 \theta \rangle = 0.867$ . Target states can also be reached to within better than 0.5%.

By starting all simulations from the ground rotational state, we have in fact made the approximation of a zero initial rotational temperature. From previous work on laser-induced alignment and orientation,<sup>28,29,30,31,32</sup> it is known that considering a higher, experimentally more realistic initial rotational temperature will lead to an important decrease in the amount of orientation/alignment obtained. However, additional studies<sup>28,29</sup> have also shown that the same basic mechanisms for orientation are at work for  $T > 0$  K, and thus that the results obtained here should be transferable to higher temperatures in a qualitative way. At the same time, we note that there is an intrinsic limit on the amount of orientation/alignment



that can be achieved when considering a *unitary* evolution of mixed states,<sup>33</sup> i.e., in the absence of any coupling to an environment.

As a rigid rotor model was used, this study did not take into account any vibrational excitation, which could hinder or enhance the orientation/alignment obtained. By including vibrations into the model, it is possible to use different control paths not involving direct rotational excitation, enabling the choice of infra-red lasers as control fields.<sup>34,35,36</sup> Vibration-rotation coupling can also lead to cross-revivals of vibrational wave packets.<sup>37,38</sup> Future work will thus take into account the vibration of the molecule.

---

\* Electronic address: salomon@ann.jussieu.fr

† Electronic address: claudedion@tp.umu.se

‡ Electronic address: gabriel.turinici@inria.fr

- <sup>1</sup> P. R. Brooks, *Science* **193**, 11 (1976).
- <sup>2</sup> M. G. Tenner, E. W. Kuipers, A. W. Kleyn, and S. Stolte, *J. Chem. Phys.* **94**, 5197 (1991).
- <sup>3</sup> J. J. McClelland, R. E. Sejolt, E. C. Palm, and R. J. Celotta, *Science* **262**, 877 (1993).
- <sup>4</sup> T. Seideman, *Phys. Rev. A* **56**, R17 (1997).
- <sup>5</sup> B. K. Dey, M. Shapiro, and P. Brumer, *Phys. Rev. Lett.* **85**, 3125 (2000).
- <sup>6</sup> A. D. Bandrauk and H. Z. Lu, *Phys. Rev. A* **68**, 043408 (2003).
- <sup>7</sup> R. de Nalda, E. Heesel, M. Lein, N. Hay, R. Velotta, E. Springate, M. Castillejo, and J. P. Marangos, *Phys. Rev. A* **69**, 031804(R) (2004).
- <sup>8</sup> K. F. Lee, D. M. Villeneuve, P. B. Corkum, and E. A. Shapiro, *Phys. Rev. Lett.* **93**, 233601 (2004).
- <sup>9</sup> H. Stapelfeldt and T. Seideman, *Rev. Mod. Phys.* **75**, 543 (2003).
- <sup>10</sup> D. Tannor, V. Kazakov, and V. Orlov, in *Time Dependent Quantum Molecular Dynamics*, edited by J. Broeckhove and L. Lathouwers (Plenum Press, New York, 1992), pp. 347–360.
- <sup>11</sup> W. Zhu and H. Rabitz, *J. Chem. Phys.* **109**, 385 (1998).
- <sup>12</sup> Y. Maday and G. Turinici, *J. Chem. Phys.* **118**, 8191 (2003).
- <sup>13</sup> R. S. Judson, K. K. Lehmann, H. Rabitz, and W. S. Warren, *J. Mol. Spectrosc.* **223**, 425 (1990).
- <sup>14</sup> R. S. Judson and H. Rabitz, *Phys. Rev. Lett.* **68**, 1500 (1992).
- <sup>15</sup> J. Karczmarek, J. Wright, P. Corkum, and M. Ivanov, *Phys. Rev. Lett.* **82**, 3420 (1999).

- <sup>16</sup> D. M. Villeneuve, S. A. Aseyev, P. Dietrich, M. Spanner, M. Y. Ivanov, and P. B. Corkum, *Phys. Rev. Lett.* **85**, 542 (2000).
- <sup>17</sup> M. Spanner and M. Y. Ivanov, *J. Chem. Phys.* **114**, 3456 (2001).
- <sup>18</sup> M. Spanner, K. M. Davitt, and M. Y. Ivanov, *J. Chem. Phys.* **115**, 8403 (2001).
- <sup>19</sup> N. V. Vitanov and B. Girard, *Phys. Rev. A* **69**, 033409 (2004).
- <sup>20</sup> A. Ben Haj-Yedder, A. Auger, C. M. Dion, E. Cancès, A. Keller, C. Le Bris, and O. Atabek, *Phys. Rev. A* **66**, 063401 (2002).
- <sup>21</sup> T. Seideman, *Phys. Rev. Lett.* **83**, 4971 (1999).
- <sup>22</sup> D. Sugny, A. Keller, O. Atabek, D. Daems, C. M. Dion, S. Guérin, and H. R. Jauslin, *Phys. Rev. A* **69**, 033402 (2004).
- <sup>23</sup> D. Sugny, A. Keller, O. Atabek, D. Daems, C. M. Dion, S. Guérin, and H. R. Jauslin, *Phys. Rev. A* **71**, 063402 (2005).
- <sup>24</sup> Y. Maday, J. Salomon, and G. Turinici, in *Proceedings of the LHMNLC03 IFAC Conference* (2003), pp. 321–324.
- <sup>25</sup> Y. Maday, J. Salomon, and G. Turinici, *Numer. Math.* (to appear).
- <sup>26</sup> M. B. Priestley, *Spectral Analysis and Time Series* (Academic Press, San Diego, 1981).
- <sup>27</sup> C. M. Dion, A. Keller, and O. Atabek, *Phys. Rev. A* (to appear), arXiv:physics.chem-ph/0505060.
- <sup>28</sup> C. M. Dion, A. Ben Haj-Yedder, E. Cancès, C. Le Bris, A. Keller, and O. Atabek, *Phys. Rev. A* **65**, 063408 (2002).
- <sup>29</sup> M. Machholm and N. E. Henriksen, *Phys. Rev. Lett.* **87**, 193001 (2001).
- <sup>30</sup> J. Ortigoso, M. Rodríguez, M. Gupta, and B. Friedrich, *J. Chem. Phys.* **110**, 3870 (1999).
- <sup>31</sup> T. Seideman, *J. Chem. Phys.* **115**, 5965 (2001).
- <sup>32</sup> M. Machholm, *J. Chem. Phys.* **115**, 10724 (2001).
- <sup>33</sup> D. Sugny, A. Keller, O. Atabek, D. Daems, C. M. Dion, S. Guérin, and H. R. Jauslin, (submitted).
- <sup>34</sup> C. M. Dion, A. Keller, O. Atabek, and A. D. Bandrauk, *Phys. Rev. A* **59**, 1382 (1999).
- <sup>35</sup> C. M. Dion, A. D. Bandrauk, O. Atabek, A. Keller, H. Umeda, and Y. Fujimura, *Chem. Phys. Lett.* **302**, 215 (1999).
- <sup>36</sup> K. Hoki and Y. Fujimura, *Chem. Phys.* **267**, 187 (2001).
- <sup>37</sup> T. Hansson, *Phys. Rev. A* **61**, 033404 (2000).

- <sup>38</sup> S. Wallentowitz, I. A. Walmsley, L. J. Waxer, and T. Richter, J. Phys. B: At., Mol. Opt. Phys. **35**, 1967 (2002).

$J$	$c_J^o$	$c_J^a$
0	0.344185	0.413914
1	0.540216	0.
2	0.563165	0.744364
3	0.456253	0.
4	0.253736	0.524021

TABLE I: Expansion coefficients [see Eq. (2)] for the target states  $\psi_{\text{target}}$  corresponding to maximum orientation,  $c_J^o$ , and alignment,  $c_J^a$ , when the rotational excitation is restricted to  $J_{\text{max}} = 4$ .

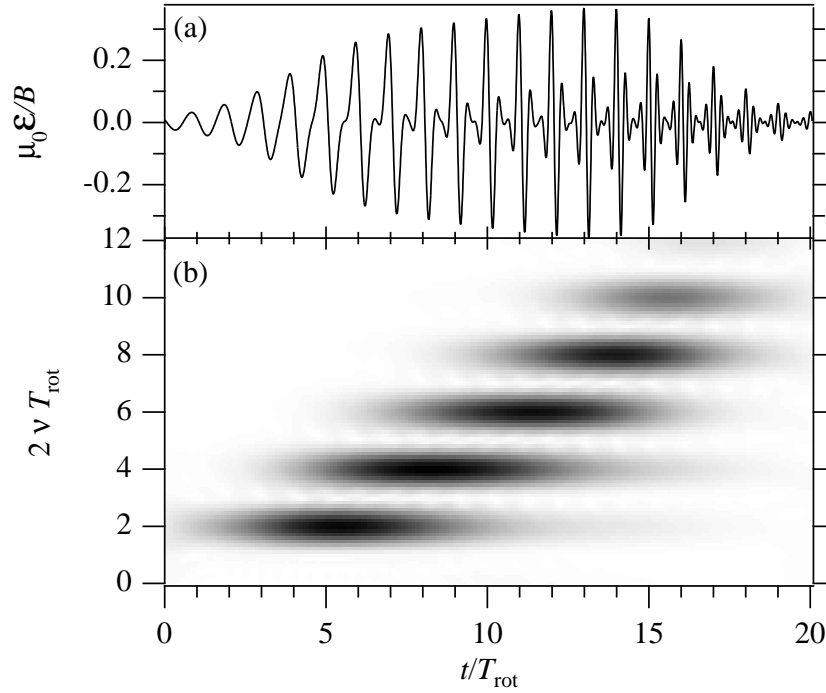


FIG. 1: (a) Electric field obtained with criterion  $\mathcal{J}_1$  for the optimization of  $\langle \cos \theta \rangle$ . (b) Short-time Fourier transform of the field in (a).

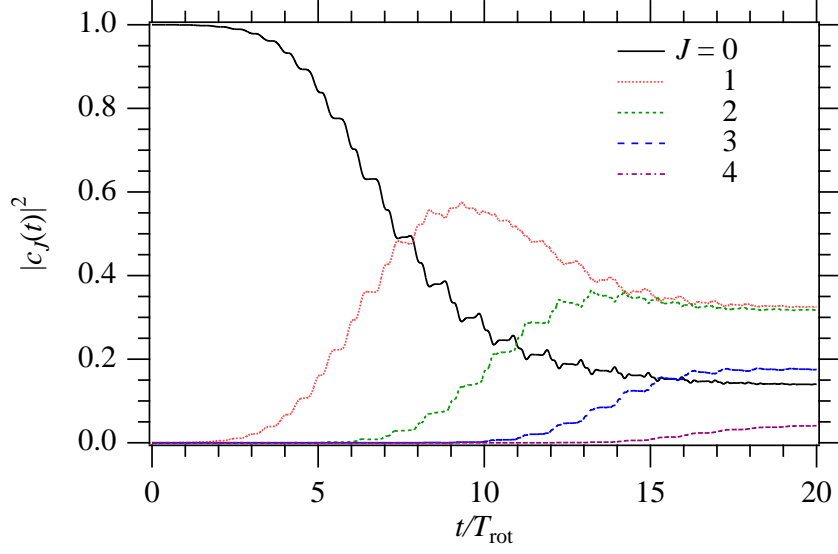


FIG. 2: Time evolution of the population of rotational states of a rigid rotor interacting with the electric field given in Fig. 1(a).

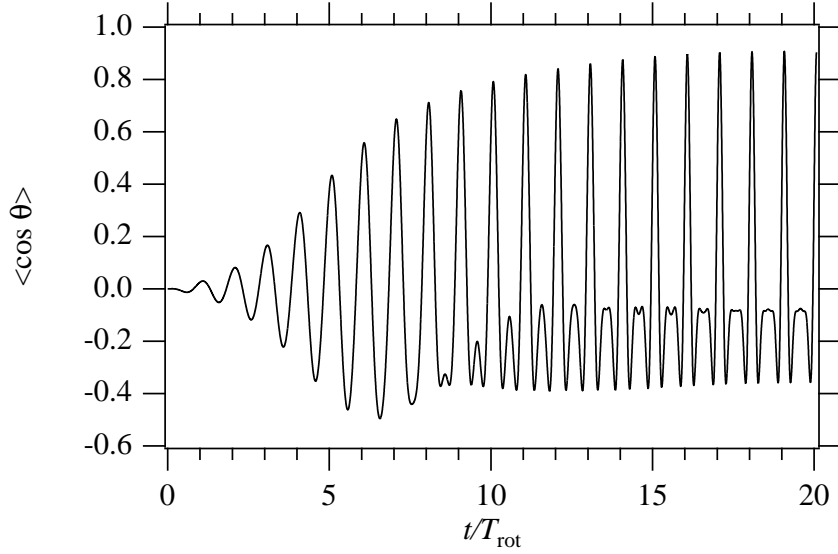


FIG. 3: Orientation, as measured by  $\langle \cos \theta \rangle$ , obtained for a rigid rotor interacting with the electric field given in Fig. 1(a). The field-free evolution is then periodic with period  $T_{\text{rot}}$ .

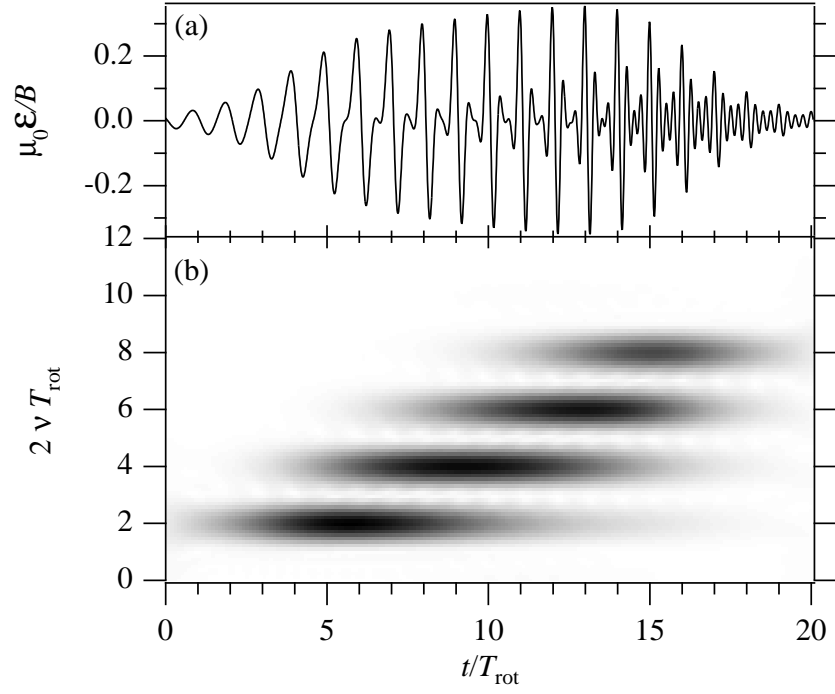


FIG. 4: (a) Electric field obtained with criterion  $\mathcal{J}_2$  for the optimization of the projection of wave function on the target  $\psi_{\text{target}}$  corresponding to orientation (see Tab. I). (b) Short-time Fourier transform of the field in (a).

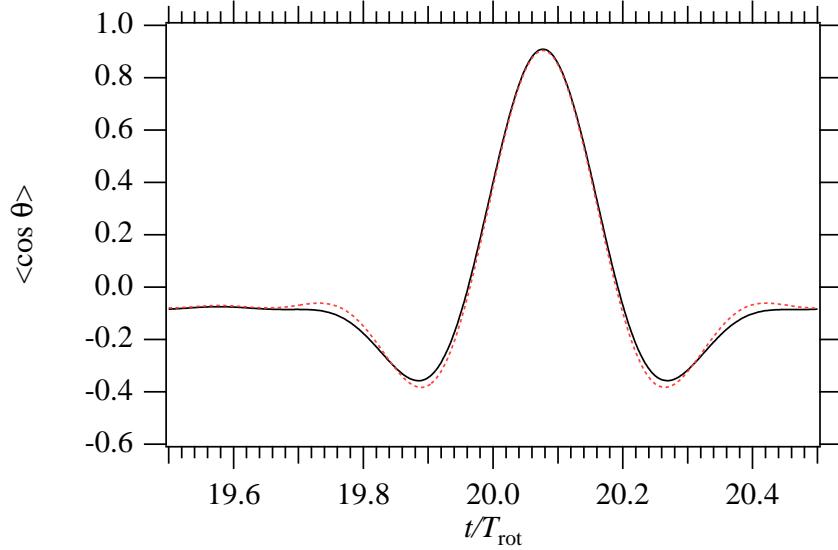


FIG. 5: Orientation, as measured by  $\langle \cos \theta \rangle$ , obtained for the interaction with the electric field given in Fig. 1(a) (solid line) and Fig. 4(a) (dashed line). The field-free evolution is then periodic with period  $T_{\text{rot}}$ .

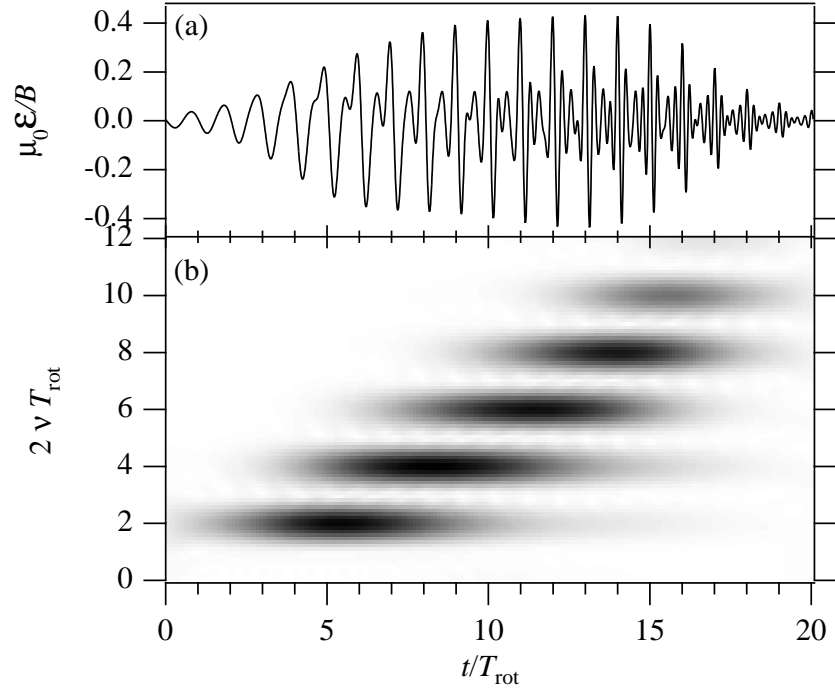


FIG. 6: Same as Fig. 1, but for the optimization of  $\langle \cos^2 \theta \rangle$ .

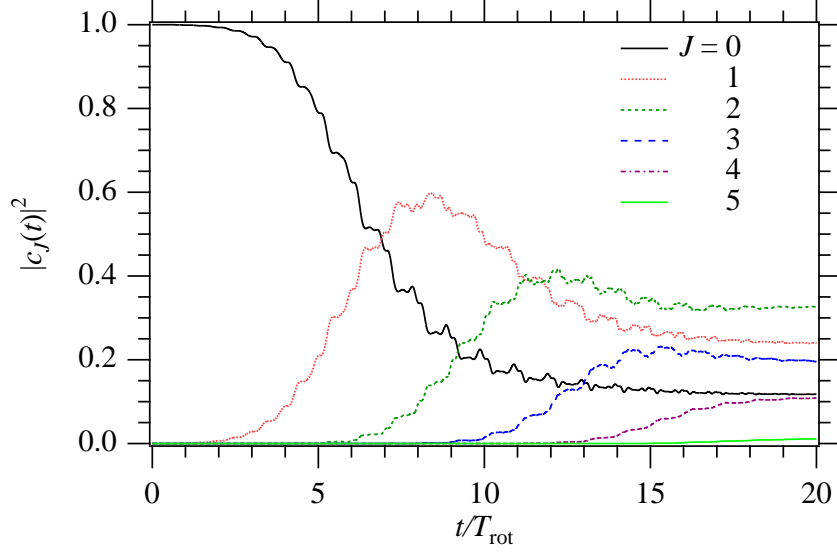


FIG. 7: Time evolution of the population of rotational states of a rigid rotor interacting with the electric field given in Fig. 6(a).

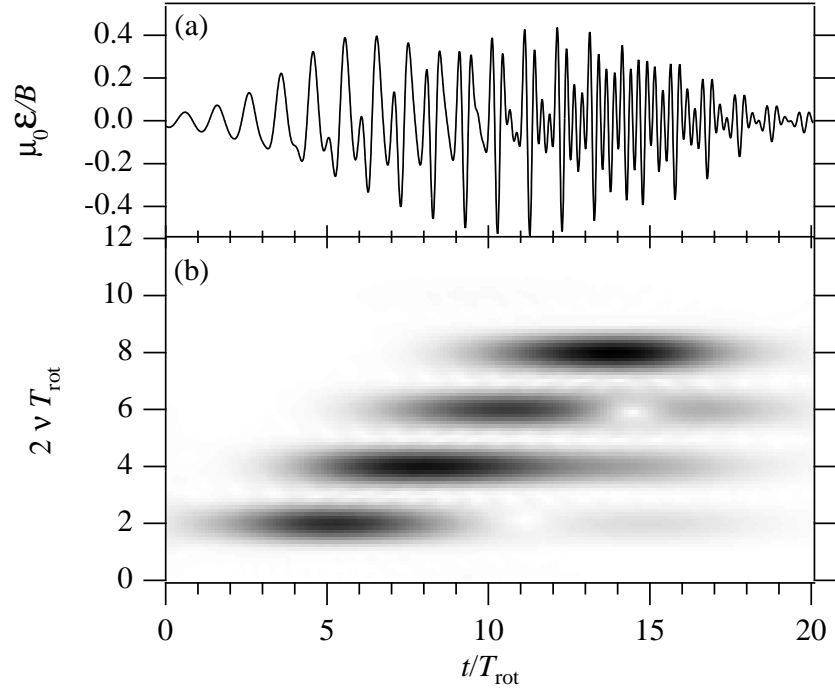


FIG. 8: Same as Fig. 4, but for the optimization of the projection of wave function on the target  $\psi_{\text{target}}$  corresponding to alignment (see Tab. I).

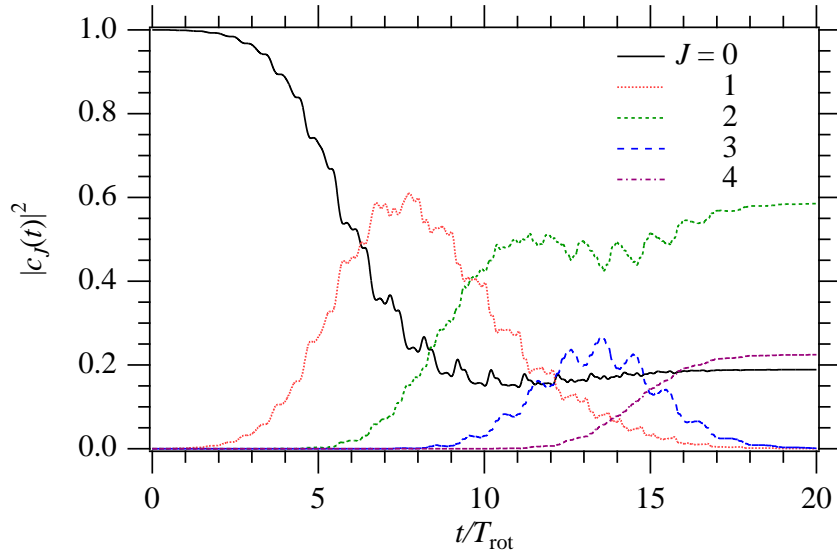


FIG. 9: Time evolution of the population of rotational states of a rigid rotor interacting with the electric field given in Fig. 8(a).



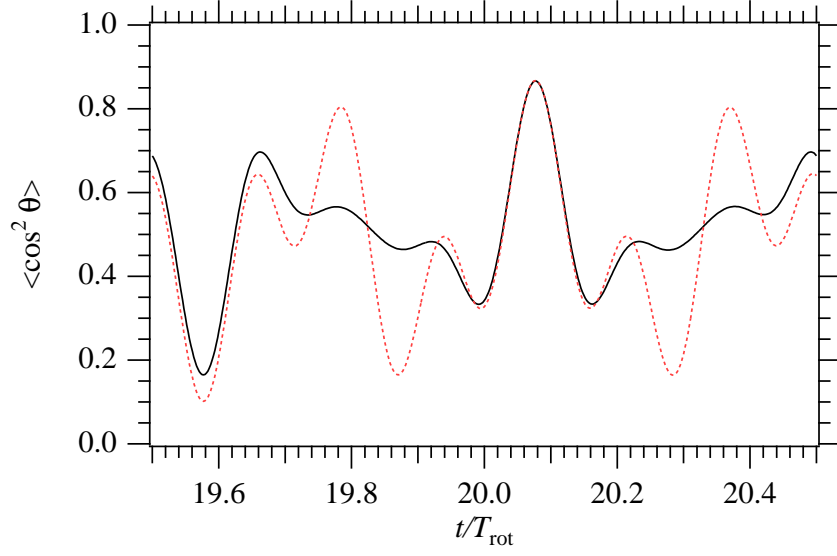


FIG. 10: Alignment, as measured by  $\langle \cos^2 \theta \rangle$ , obtained for the interaction with the electric field given in Fig. 6(a) (solid line) and Fig. 8(a) (dashed line). The field-free evolution is then periodic with period  $T_{\text{rot}}$ .